Euler and Navier-Stokes Solutions for Supersonic Shear Flow past a Circular Cylinder

Ajay Kumar* and M. D. Salas†
NASA Langley Research Center, Hampton, Virginia

Euler and Navier-Stokes solutions of the supersonic shear flow past a circular cylinder are obtained. These solutions are used to study the basic flow structure around the cylinder. Both the inviscid and viscous calculations show the formation of a large recirculating flow region around the front stagnation point. The calculations further show that the overall size of the recirculating region is approximately the same for the Euler and Navier-Stokes solutions, but the inside structure is quite different. The inviscid flow shows only one vortex, whereas the viscous flow shows two vortices inside the recirculating flow region. The inner vortex in the Navier-Stokes solution is formed primarily due to the viscous effects near the body surface and its size depends upon the Reynolds number. It is found that, with increasing Reynolds number, the inner vortex diminishes in size and the Navier-Stokes solution asymptotically approaches the Euler solution. These results indicate that the Euler equations may correctly predict certain high Reynolds number separation phenomena in flows with a natural inviscid vorticity source.

Nomenclature

c_f = skin friction, nondimensionalized by $\rho'_{\infty 1} U'^2_{\infty 1}/2$
c_h = surface heating rate, nondimensionalized by $\rho'_{\infty 1} U'^3_{\infty 1}/2$
d_{stag} = distance of stagnation point along the $\theta = 0$ deg line measured from the body surface, d'_{stag}/R'
M = Mach number
n = normal coordinate, n'/R'
p = pressure, $p'/\rho'_{\infty 1} U'^2_{\infty 1}$
R' = cylinder radius (assumed unity)
Re = Reynolds number
s = tangential distance, s'/R'
u = tangential velocity, $u'/U'_{\infty 1}$
U_0 = velocity just behind the shock at the $\theta = 0$ deg line, $U'_0/U'_{\infty 1}$
U'_∞ = freestream velocity
v = normal velocity, $v'/U'_{\infty 1}$
ρ = density, $\rho'/\rho'_{\infty 1}$
θ = body angle measured from the symmetry line
ω = vorticity

Superscript

$( )'$ = dimensional quantities

Subscripts

1 = conditions at the symmetry line
2 = conditions at unit height
ω = surface conditions
∞ = freestream conditions

Introduction

WITH the increasing effort to obtain numerical solutions of the Euler equations, the occurrence of "inviscid separation" has become a de facto phenomenon. Inviscid separation has been observed in numerical calculations of flow past circular cylinders,[1] circular cones,[2] delta wings,[3,4] airfoils,[5] and rearward-facing steps.[6] However, the legitimacy of such a phenomenon as a valid solution of the differential equations has been the focus of a growing controversy.[7] Theoretical studies by Fraenkel[8] and Küchemann[9] have demonstrated that inviscid separation can occur in rotational flows as a result of the premature retardation of the surface velocity caused by vorticity in the flow. The controversy, therefore, should not center on the validity of inviscid separation as such, but on the appropriateness of the mechanism that generates the vorticity and on whether the solutions are unique and, therefore, whether the problem is well posed. Vorticity can be introduced in an inviscid flow through initial and boundary conditions; this is how Fraenkel and Küchemann introduced it in their studies of separation. It can also be produced by shock waves and, in some cases, by geometrical singularities where the requirement of a smooth solution leads to the formation of a vortex sheet. Unfortunately, vorticity can also be introduced when problems are solved numerically due to the artificial dissipation inherent or otherwise forcefully added to a numerical scheme. Numerical calculations that exhibit inviscid separation must, therefore, be carefully assessed to determine their validity. The question of uniqueness arises from the fact that the "steady" Euler equations are known to have multiple solutions.[10] However, it is not clear if all of these multiple solutions are stable or if these can be obtained as asymptotic limits of the time-dependent Euler equations.

To shed some light on the inviscid separation phenomenon, the present paper investigates the flow set up by a supersonic sheared freestream impinging on a circular cylinder. A schematic of the flow is shown in Fig. 1. The numerical solution of the Euler equations for this flow exhibits a large region of recirculating flow ahead of the usual front stagnation point. The appearance of the recirculating flow has been obtained by several numerical methods[11,12] and has also been observed experimentally.[13] The numerical studies in Refs. 11 and 12 must be considered of a preliminary nature. In the present study, the phenomenon is investigated in detail as a limiting solution of the Navier-Stokes equations for very large Reynolds numbers. The problem is ideally suited to this type of investigation for two reasons: First, the bulk of the vorticity is introduced as a boundary condition; and second, the separation occurs along a symmetry line, not along a solid surface. The second reason is important because on a solid surface the nature of inviscid separation is significantly different from the usual boundary-layer separation. For example, the pressure level at an inviscid separation point on a smooth solid surface is its stagnation value, while the usual

Received Dec. 30, 1983; presented as Paper 84-0339 at the AIAA 22nd Aerospace Sciences Meeting, Reno, Nev., Jan. 9-12, 1984; revision received April 4, 1984. This paper is declared a work of the U.S. Government and therefore is in the public domain.

*Aerospace Engineer, Computational Methods Branch, High Speed Aerodynamics Division. Member AIAA.

†Research Scientist, Theoretical Aerodynamics Branch, Transonic Aerodynamics Division. Associate Fellow AIAA.

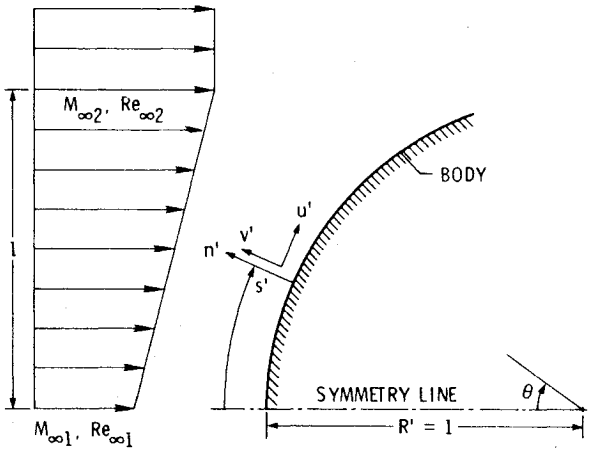

Fig. 1 Coordinate system for supersonic shear flow past a circular cylinder.

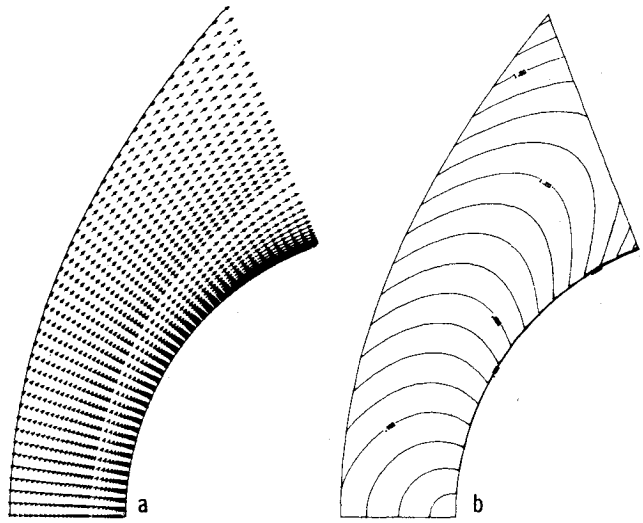

Fig. 2 Uniform supersonic flow past a circular cylinder: a) velocity vector field; b) Mach number contours.

boundary layer separates at lower values of pressure. However, for the problem under investigation, both the inviscid and viscous separations occur at stagnation pressure levels.

The purpose of the paper is, therefore, an investigation of the limiting solution of the Navier-Stokes equations for high Reynolds numbers and an assessment of the relevance of the Euler solutions for supersonic shear flow past a circular cylinder.

Outline of Method

In the present analysis, inviscid and viscous solutions are obtained by solving the Euler and Navier-Stokes equations, respectively. The equations are solved in the body-oriented coordinate system as shown in Fig. 1. The code described in Ref. 14 is used for the inviscid flow, whereas for the viscous flow, the code developed in Ref. 15 is used with some modifications. In both cases, the independent variables are transformed such that both the bow shock wave and the body surface become boundary mesh lines. Flow conditions behind the shock, forming an outer boundary of the region of interest, are obtained by using the Rankine-Hugoniot relations. The shock-fitting approach removes most of the artificial viscosity usually introduced with shock-capturing schemes. In the viscous calculations, a second transformation is also used that further maps the computational plane to yet another plane to allow higher resolution near the body. This is required to adequately resolve the viscous effects near the body.

Both the viscous and inviscid codes use MacCormack's two-step, finite difference method[16] to solve the flow behind the shock to the body. This method finds the steady-state solution as the time-asymptotic solution of the time-dependent governing equations. The Euler equations are solved in nonconservative form and require no explicit artificial damping. Since the shock wave is fitted rather than captured, use of a nonconservative form of the equations should not affect the results. The Navier-Stokes equations are solved in conservative form and require additional explicit artificial damping. The damping used is of fourth order and is added only once per time step after completing both the predictor and the corrector steps. An attempt has been made to assess the effect of the artificial damping and to keep the contribution from this additional damping term to a minimum.

Discussion of Results

Detailed results are presented here for inviscid as well as viscous flow with varying freestream shear and Reynolds number. A uniform grid of 27 points along the body and 21 points normal to the body is used for inviscid calculations. Viscous calculations are made with a grid of 41 points along the body and 51 points normal to the body. Grid points are uniformly spaced along the body, but are highly stretched in the normal direction to cluster more points near the surface. In order to contrast the flow structure of the uniform flow with that of the freestream shear, Fig. 2 shows the Navier-Stokes solution for a uniform freestream at Mach 10, i.e., $M_{\infty 1} = M_{\infty 2} = 10$. The freestream Reynolds number is 0.766×10^6. Figure 2a shows the velocity vector field and Fig. 2b the Mach number contours. (For clarity, in all of the velocity vector plots for viscous flow shown in this paper, every other grid point along lines normal to the surface is plotted for the first 33 points and thereafter every grid point is plotted.) As expected, Fig. 2a shows no recirculating flow region. The shock standoff distance is seen to increase with increasing distance along the body.

Calculations are then made for a case where the freestream has linear shear up to a unit height from the axis of symmetry and then becomes uniform. The freestream Mach number varies from 10 at the symmetry line to 18 at the unit height, i.e., $M_{\infty 1} = 10$ and $M_{\infty 2} = 18$. The freestream Reynolds number varies from 0.39×10^6 at the symmetry line to 0.7×10^6 at the unit height. Freestream static pressure, density, and temperature were assumed uniform. Figures 3a, 3b, and 3c show the velocity vector field, Mach number contours, and vorticity contours, respectively, for the Navier-Stokes solution. In contrast to the results shown in Fig. 2, this flow shows a large recirculating flow region around the front stagnation point with relatively low energy. As can be seen from the Mach number contours, the flow in the recirculating region has Mach numbers less than 0.1. The recirculating flow region pushes the shock outward, thus significantly increasing the shock standoff distance near the stagnation point. The flow is seen to reattach to the body at about $\theta = 40$ deg.

The Euler solution for the same freestream shear case is shown in Fig. 4. It is seen from Fig. 4a that the Euler solution also shows a recirculating flow region around the front stagnation point, which is approximately of the same size as for the viscous flow. This is due to the fact that, for this problem, the vorticity in the flow causing the recirculating flow region is generated primarily by the freestream shear and secondarily by the bow shock wave. Both of these sources are present in the inviscid and viscous flows. In the case of the viscous flow, vorticity is also generated within the shear layer along the symmetry line and within the boundary layer near the body surface. In the present calculations, it is found that the vorticity due to viscous effects has little impact on the overall size of the recirculating region, but the internal structure of the recirculating region as such is significantly

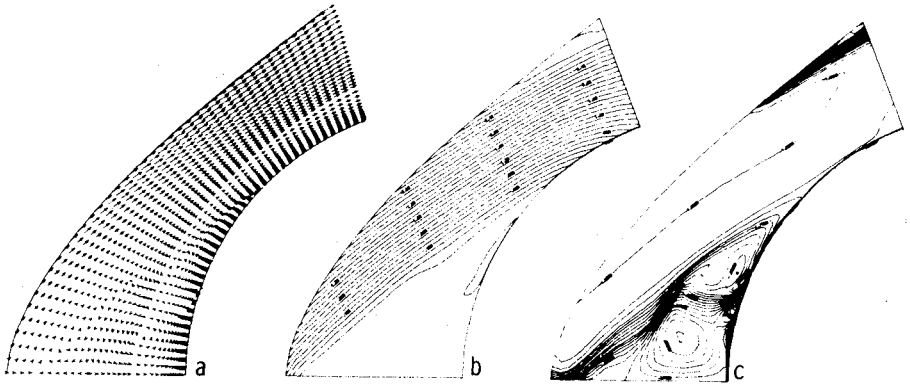

Fig. 3 Navier-Stokes solution for the supersonic shear flow at $Re_{\infty 1} = 0.39 \times 10^6$: a) velocity vector field; b) Mach number contours; c) vorticity contours.

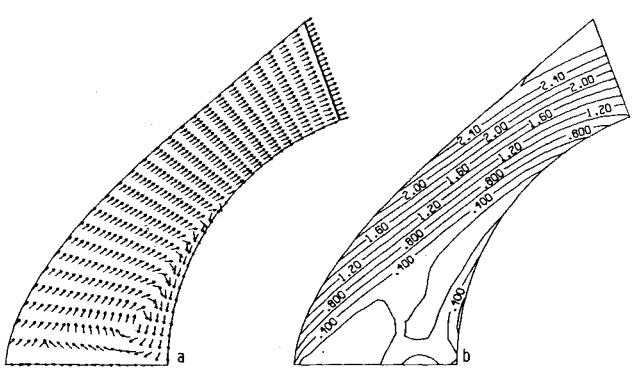

Fig. 4 Euler solution for the supersonic shear flow: a) velocity vector field; b) Mach number contours.

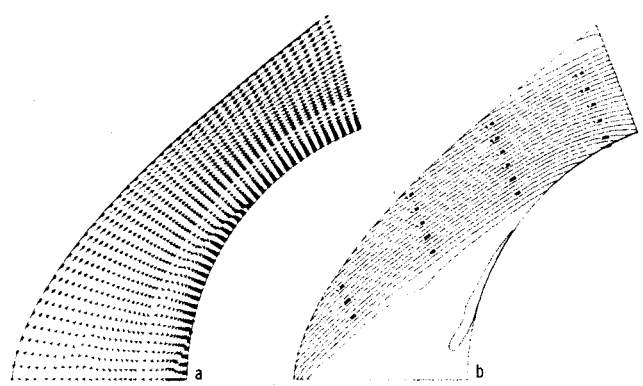

Fig. 6 Navier-Stokes solution for the supersonic shear flow at $Re_{\infty 1} = 0.766 \times 10^6$: a) velocity vector field; b) Mach number contours.

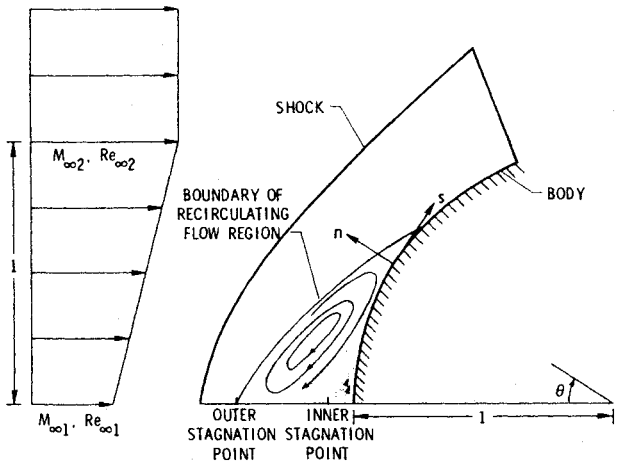

Fig. 5 Schematic of viscous supersonic shear flow past a circular cylinder.

altered. Figures 3a and 3c show that there are two counterrotating vortices inside the recirculating region. The inner vortex, not present in the inviscid flow, is apparently formed by the action of the viscous effects near the body surface. The formation of this inner vortex was not observed by Lin et al.[12] in their Navier-Stokes solution. The presence of two vortices in the viscous flow gives rise to two additional stagnation points along the symmetry line other than the stagnation point on the body. The inviscid flow has only one additional stagnation point along the symmetry line. Based on the present calculations, the basic structure of the viscous supersonic shear flow past a circular cylinder can be drawn schematically as shown in Fig. 5. The two additional stagnation points on the axis of symmetry are marked as inner and outer stagnation points.

Figure 6 shows the Navier-Stokes results for another case in which the freestream shear is kept the same as in the preceding case, but the freestream Reynolds number is increased significantly by reducing the freestream temperature. The freestream Reynolds number for this case changes from 0.766×10^6 at the symmetry line to 1.38×10^6 at the unit height. It can be seen from Fig. 6 that the change in Reynolds number has very little effect on the overall size of the recirculating region, but that the size of the inner vortex is significantly reduced compared to that shown in Fig. 3a. From these results, it can be concluded that the overall size of the recirculating region depends mainly upon the inviscid vorticity generated by the freestream shear and bow shock wave. But, the size of the inner vortex depends upon both the inviscid vorticity and freestream Reynolds number. From this dependence on freestream Reynolds number, it can be concluded that the inner vortex arises from the action of viscous forces near the body surface and its size depends upon the viscosity of the fluid.

In order to investigate the behavior of the Navier-Stokes solution with increasing Reynolds number, a number of calculations are made in which the freestream shear is held fixed ($M_{\infty 1} = 10$, $M_{\infty 2} = 18$), but the Reynolds number is gradually increased. Figure 7 shows a plot of the distances of the inner and outer stagnation points (d_{stag}) measured from the body surface against the reciprocal of the freestream Reynolds number $Re_{\infty 1}$. Inviscid values are also marked on this figure by symbol X on the vertical axis, which corresponds to infinite Reynolds number. It is seen that the distance of the outer stagnation point remains practically constant at all Reynolds numbers and its value is about the same as for the inviscid flow. The distance of the inner stagnation point also does not change significantly up to about $Re_{\infty 1} = 0.5 \times 10^6$, but with further increase in Reynolds number, the distance drops rather quickly and, in fact, it appears from the figure as though it will approach zero asymptotically at very high Reynolds numbers. It is presently not known why the distance of the inner stagnation point suddenly drops at a Reynolds number of 0.6×10^6. The phenomenon, however, appears to be physical rather than

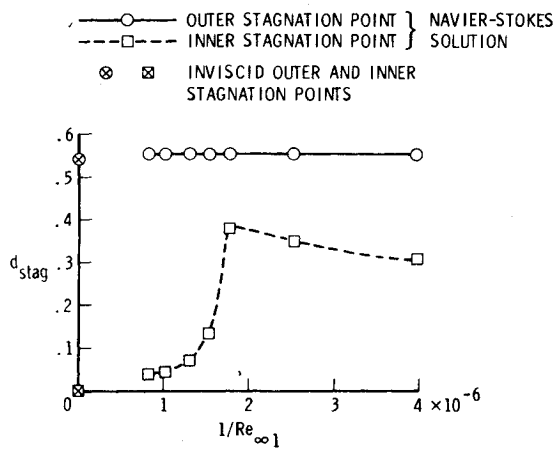

Fig. 7 Variation of outer and inner stagnation point distances with Reynolds number.

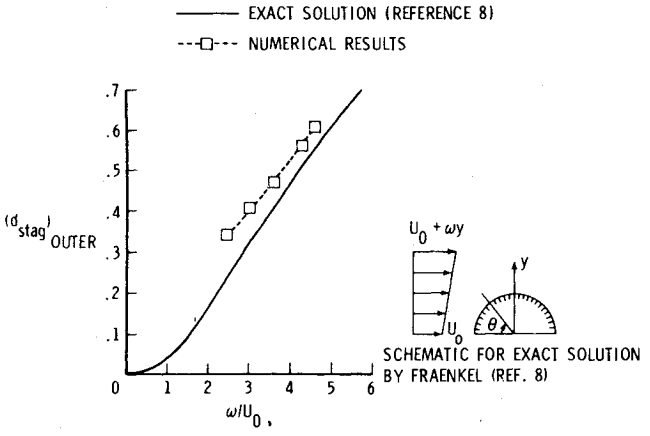

Fig. 8 Variation of outer stagnation point distance with vorticity.

numerical, since the numerical effects should not be very different for Reynolds numbers of 0.56×10^6 and 0.65×10^6, between which most of the drop in distance occurs. Although no attempt was made to calculate the flow at much higher Reynolds numbers due to the large grid and computer resource requirements, Fig. 7 does indicate that the Navier-Stokes solution approaches the Euler solution in the limit of vanishing viscous effects. The results also show that the Euler equations may well predict the separation phenomenon at high Reynolds numbers in flows where it occurs primarily due to the inviscid vorticity.

In order to further establish the validity of the present calculations, the extent of the recirculation region along the symmetry line is compared with an exact solution of the shear flow past a circular cylinder. Although the exact solution developed by Fraenkel[8] is for an inviscid, incompressible flow with constant vorticity, the comparison has some validity due to the fact that, in the present problem, the flow behind the shock is basically inviscid and incompressible (Mach number is less than 0.3, see Figs. 3 and 6) along the symmetry line. Shown in Fig. 8 is the distance of the outer stagnation point from the surface plotted against the vorticity ω. A schematic of the exact problem is also shown in the figure. In the present calculation, ω is the vorticity just behind the shock at the symmetry line. It is varied by changing the freestream shear. Figure 8 shows that the present calculations are in good agreement with the exact solution, considering the fact that the vorticity behind the shock in the present problem is not constant.

Figure 9 shows a plot of the angle at which the recirculating flow region reattaches to the body. It is also plotted against the vorticity ω. It is seen that the reattachment angle increases

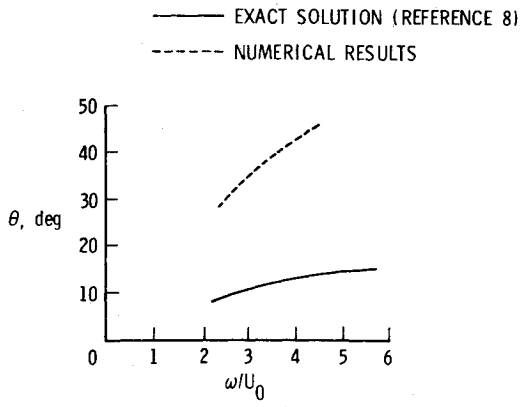

Fig. 9 Variation of reattachment angle with vorticity.

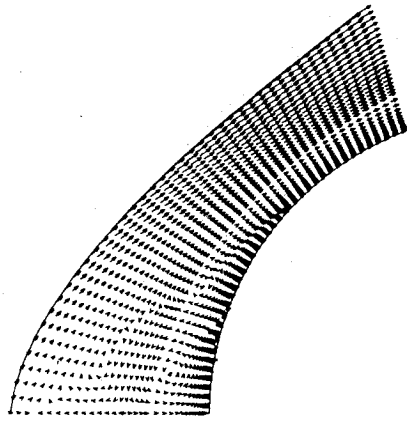

Fig. 10 Effect of local time step on the structure of recirculating flow region.

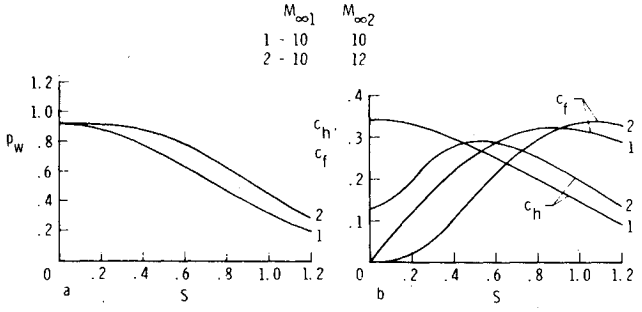

Fig. 11 Effect of freestream shear on surface quantities: a) surface pressure distribution; b) surface heat-transfer rate and skin-friction distribution.

with the increase in vorticity. The reattachment angle for the inviscid, incompressible flow with constant vorticity[8] is also shown in the figure. Although the conditions of present calculations near reattachment differ very significantly from those of Fraenkel,[8] the exact solution from Ref. 8 is included for the sake of completeness. The significant deviation can be expected because, as the flow accelerates over the front of the body, compressibility effects become more important. In addition, and perhaps more importantly, the vorticity is not constant and, in particular, the vorticity generated at the body surface due to viscosity also affects the reattachment angle.

In calculating the preceding solutions, care was taken to keep the influence of numerics as small as possible. Checks were made to insure that the converged solution did not depend on initial conditions or on the location of the outflow boundary. Since numerical dissipation also introduces vorticity in the flow, which affects the recirculating flow region, attempts were made to keep the explicit artificial damping coefficient to the smallest value possible. Use of a local time

step to speed up the convergence was avoided because it was found to affect the structure of the recirculating flow region. Figure 10 shows the results obtained by using a local time step for the case discussed in Fig. 6. It is seen that in comparison to Fig. 6a, where a global minimum time step is used, Fig. 10 shows a much larger size of the inner vortex. This change in the structure of the recirculating flow region may be because the steady-state solution using the MacCormack scheme depends on Δt. Further, the use of local Δt may also affect the amount of artificial dissipation. To avoid these problems, all of the results presented earlier were obtained with the global minimum time step.

Finally, although the emphasis of the present study has been mainly on the basic flow structure, Fig. 11 shows the effects of freestream shear on surface pressure, heating rate, and skin friction. It is seen that all the surface quantities are significantly affected by the freestream shear. Even a moderate shear of 10-12 in Mach number changes the surface pressure, heating rate, and skin friction considerably.

Conclusions

Time-asymptotic solutions of the Euler and Navier-Stokes equations are obtained to study the basic flow structure of the supersonic shear flow past a circular cylinder. In obtaining these solutions, precautions are taken to keep the influence of numerics to a minimum. Both the inviscid and viscous calculations show the formation of a large recirculating flow region around the front stagnation point. The calculations further show that the overall size of the recirculating region is approximately the same for the Euler and Navier-Stokes solutions, but that the inside structure is quite different. The inviscid flow shows only one vortex, whereas the viscous flow shows two vortices inside the recirculating flow region. The inner vortex in the Navier-Stokes solution is formed primarily due to the viscous effects near the body surface and its size depends upon the Reynolds number. It is found that with increasing Reynolds numbers, the inner vortex diminishes in size and the Navier-Stokes solution asymptotically approaches the Euler solution. These results indicate that the Euler equations may correctly predict certain high Reynolds number separation phenomena in flows with a natural inviscid vorticity source.

References

[1] Salas, M. D., "Recent Developments in Transonic Euler Flow Over a Circular Cylinder," *Mathematics and Computers in Simulation*, Vol. XXV, 1983, pp. 232-236.

[2] Marconi, F., "The Spiral Singularity in Supersonic Inviscid Flow Over a Cone," AIAA Paper 83-1665, June 1983.

[3] Rizzi, A., Eriksson, L. E., Schmidt, W., and Hitzel, S., "Numerical Solutions of the Euler Equations Simulating Vortex Flows Around Wings," AGARD CPP-342, April 1983.

[4] Raj, P. and Sikora, J. S., "Free Vortex Flows: Recent Encounters with an Euler Code," AIAA Paper 84-0135, Jan. 1984.

[5] Barton, J. T. and Pulliam, T. H., "Airfoil Computation at High Angles of Attack, Inviscid and Viscous Phenomena," AIAA Paper 84-0524, Jan. 1984.

[6] Schmidt, W. and Jameson, A., "Euler Solutions as Limits of Infinite Reynolds Number for Separation Flows with Vortices," *8th International Conference on Numerical Methods in Fluid Dynamics*, Springer-Verlag, New York, June 28-July 2, 1982, pp. 468-473.

[7] Garabedian, P. R., "Nonparametric Solutions of the Euler Equations for Steady Flow," *Communications on Pure and Applied Mathematics*, Vol. 36, 1983, pp. 529-535.

[8] Fraenkel, L. E., "On Corner Eddies in Plane Inviscid Shear Flow," *Journal of Fluid Mechanics*, Vol. 11, 1961, pp. 400-406.

[9] Küchemann, D., "Inviscid Shear Flow Near the Trailing Edge of an Airfoil," *Zeitschrift fuer Flugwissenschaften*, Vol. 15, 1977, pp. 292-294.

[10] Childress, S., "Solutions of Euler's Equations Containing Finite Eddies," *Physics of Fluids*, Vol. 9, May 1966, pp. 860-872.

[11] Hussaini, M. Y. and Zang, T. A., "Spectral Multi-Grid Method and Spectral Solutions to Compressible Flows," ICASE Rept. 82-40, Dec. 1982.

[12] Lin, T. C., Reeves, B. L., and Siegelman, D., "Blunt-Body Problem in Nonuniform Flow Fields," *AIAA Journal*, Vol. 15, Aug. 1977, pp. 1130-1137.

[13] Charwat, A. F., Roos, J. N., Dewey, F. C. Jr., and Hitz, J. A., "An Investigation of Separated Flows—Part 1: The Pressure Field," *Journal of the Aeronautical Sciences*, Vol. 28, June 1961, pp. 457-470.

[14] Salas, M. D., "Flow Properties for a Spherical Body at Low Supersonic Speeds," Paper presented at Symposium on Compufers in Aerodynamics, Polytechnic Institute of New York, New York, June 1979.

[15] Kumar, A. and Graves, R. A. Jr., "Numerical Solution of the Viscous Hypersonic Flow Past Blunted Cones at Angle of Attack," AIAA Paper 77-172, Jan. 1977.

[16] MacCormack, R. W., "The Effect of Viscosity in Hypervelocity Impact Cratering," AIAA Paper 69-354, 1969.